

RESEARCH PAPER

Verapamil- and state-dependent effect of 2-aminoethylmethanethiosulphonate (MTSEA) on *hK_v1.3* channels

Azadeh Nikouee, Malika Janbein and Stephan Grissmer

Institute of Applied Physiology, Ulm University, Ulm, Germany

Correspondence

Professor Dr Stephan Grissmer,
Institute of Applied Physiology,
Ulm University,
Albert-Einstein-Allee 11, 89081
Ulm, Germany. E-mail:
stephan.grissmer@uni-ulm.de

Keywords

voltage-gated potassium
channels; MTSEA reagent; C-type
inactivation; verapamil;
electrophysiology

Received

13 February 2012

Revised

14 June 2012

Accepted

19 June 2012

BACKGROUND AND PURPOSE

T-cells usually express voltage-gated *K_v1.3* channels. These channels are distinguished by their typical C-type inactivation. Therefore, to be able to rationally design drugs specific for the C-type inactivation state that may have therapeutic value in autoimmune disease therapy, it is necessary to identify those amino acids that are accessible for drug binding in C-type inactivated channels.

EXPERIMENTAL APPROACH

The influence of 2-aminoethylmethanethiosulphonate (MTSEA) on currents through wild-type human *K_v1.3* (*hK_v1.3*) and three mutant channels, *hK_v1.3_L418C*, *hK_v1.3_T419C* and *hK_v1.3_I420C*, in the closed, open and inactivated states was investigated by the patch-clamp technique.

KEY RESULTS

Currents through *hK_v1.3_L418C* and *hK_v1.3_T419C* channels were irreversibly reduced after the external application of MTSEA in the open state but not in the inactivated and closed states. Currents through *hK_v1.3_I420C* channels were irreversibly reduced in the open and inactivated states but not in the closed state. In the presence of verapamil, the MTSEA modification of *hK_v1.3_T419C* and *hK_v1.3_I420C* channels was prevented, while the MTSEA modification of *hK_v1.3_L418C* channels was unaffected.

CONCLUSION AND IMPLICATIONS

From our experiments, we conclude that the activation gate of all mutant channels must be open for modification by MTSEA and must also be open during inactivation. In addition, the relative movement of the S6 segments that occur during C-type inactivation includes a movement of the side chains of the amino acids at positions 418 and 419 away from the pore lining. Furthermore, the overlapping binding site for MTSEA and verapamil does not include position 418 in *hK_v1.3* channels.

Abbreviations

MTSEA, 2-aminoethylmethanethiosulphonate; Na-Ri, Na-Ringer solution; wt, wild-type

Introduction

The human *K_v1.3* (*hK_v1.3*), a mammalian homologue belonging to the *Shaker* subfamily (*K_v1*), is expressed in a variety of tissues including T- and B-lymphocytes (DeCoursey *et al.*, 1984; Grissmer *et al.*, 1990). The *hK_v1.3* channels are made up of four subunits. Each subunit consists of 6 transmembrane

α -helical segments S1–S6 and a membrane-re-entering P-loop (P) between S5 and S6. The S1–S4 segments act as voltage-sensor domains, while the S5–P–S6 segments form the ion-conducting pore (Long *et al.*, 2005a,b).

Voltage-gated *hK_v1.3* channels have three main functional states in response to the membrane potential. Upon hyperpolarization, *hK_v1.3* channels are in the

non-conducting closed state (C), membrane depolarizations cause conformational changes at the intracellular gate leading to the conducting open state (O). Prolonged depolarizations lead to another non-conducting state named C-type inactivated state (I), which is typical for *hK_v1.3* channels (DeCoursey *et al.*, 1984). C-type inactivation seems to be due to a constriction of the outer vestibule (Grissmer and Cahalan, 1989; Choi *et al.*, 1991; Yellen *et al.*, 1994) and/or a constriction at the selectivity filter region (Kiss and Korn, 1998; Lenaeus *et al.*, 2005; Cordero-Morales *et al.*, 2006).

New clues about the molecular model of C-type inactivation were provided by the crystal structure of *KcsA* channels in the open and inactivated states (Cuello *et al.*, 2010a,b). This model suggested that a series of consecutive structural rearrangements such as hinge bending and rotation of the TM₂ helix (equivalent to the S6 helix in *K_v1.3* channels) lead to gradual changes in the ion occupancy in the selectivity filter resulting in the prevention of the ion conduction in the inactivated state (Cuello *et al.*, 2010a,b). Investigation of the verapamil binding site revealed that pore-facing residues in the S₆ helix of the channel are in close contact with verapamil; especially A413 was detected as an important residue for the verapamil affinity (Rauer and Grissmer, 1999; Hanner *et al.*, 2001).

Previous studies in our laboratory showed that the *hK_v1.3_V417C* mutant channel could be modified in the whole-cell recording mode by the membrane-permeable 2-aminoethylmethanesulphonate (MTSEA) reagent in the open and the inactivated state but not in the closed state and the modification could be prevented by verapamil (Schmid and Grissmer, 2011). In the present study, we used similar techniques and experimental procedures to determine the verapamil- and state-dependent effect of MTSEA on three other *hK_v1.3_L418C*, *hK_v1.3_T419C* and *hK_v1.3_I420C* mutant channels. These series of amino acids 417–420, which are located in a turn of the S6 segment of the *hK_v1.3* channel, were used to identify the S6 structural rearrangement during C-type inactivation.

Methods

Cell culture

The COS-7 cell line was obtained from the Deutsche Sammlung von Mikroorganismen und Zellkulturen GmbH (DSMZ, Braunschweig, Germany, Cat. No. ACC60). COS-7 cells were cultured in Dulbecco's modified Eagle's medium containing 4.5 g·L⁻¹ glucose (Invitrogen, Carlsbad, CA, USA, Cat. No. 41966) and supplemented with 10% FBS (Thermo Fisher Scientific, Bonn, Germany, Cat. No. CH30160.02/03). Cells were incubated in a humidified incubator at 37°C and 5% CO₂.

Electrophysiology

All experiments were conducted at room temperature using the whole-cell recording mode of the patch-clamp technique (Hamill *et al.*, 1981). The external bathing solution contained 160 mM NaCl, 4.5 mM KCl, 2 mM CaCl₂, 1 mM MgCl₂ and 5 mM HEPES. The pH was adjusted to 7.4 with NaOH. The pipette filling solution (internal solution) contained 155 mM

KF, 10 mM K-EGTA, 10 mM HEPES and 1 mM MgCl₂. The pH was adjusted to 7.2 with KOH. The osmolarity of the internal and external solutions was 290–320 mOsm. Patch pipettes were pulled from 1.5 mm borosilicate glass capillaries (Science Products, Hofheim, Germany) in three stages and fire polished to resistances of 2–4 MΩ when filled with the internal solution. Currents were acquired using a HEKA EPC9 patch-clamp amplifier (HEKA Elektronik, Lambrecht, Germany) under the control of pulse software (PatchMaster v2.00, HEKA Elektronik). All currents were filtered by a 2.9 kHz Bessel filter and recorded with a sampling frequency of 1–5 kHz. Acquired currents were analysed with the HEKA FitMaster v2.00 software (HEKA Elektronik). Capacitative and leak currents were subtracted and a series resistance compensation of 75–85% was used for currents exceeding 2 nA.

The holding potential was –120 mV if not mentioned otherwise. Further data analysis was performed by the software Igor Pro 3.12 (WaveMetrics, Lake Oswego, OR, USA). If not mentioned otherwise, the number of all observations for each channel and treatment was at least five.

Molecular biology

The pRc/CMV vector containing the *hK_v1.3* wt (wild-type) potassium channel gene and a CMV promoter for protein expression in mammalian cells was a generous gift from Prof Dr O. Pongs (Institut für Neuronale Signalverarbeitung, Zentrum für Molekulare Neurobiologie, Hamburg, Germany). The mutants *hK_v1.3_L418C*, *hK_v1.3_T419C* and *hK_v1.3_I420C* used in this study were originally constructed in our laboratory by Dr Tobias Dreker by introducing the corresponding point mutation in the cloned *hK_v1.3* gene with the QuickChange site-directed mutagenesis kit (Stratagene, Amsterdam, the Netherlands). The transfection was processed using the FuGene 6 transfection reagent (Roche Molecular Biochemicals, Mannheim, Germany). One day before the transfection, cells were plated into 35 mm culture dishes. After reaching a confluence of ~80%, cells were co-transfected with ~1 μg *hK_v1.3* mutant channels DNA (L418C, T419C or I420C) and ~0.5 μg of eGFP-N1 DNA (eGFP-N1 plasmid-DNA; Clontech Laboratories, Inc., Palo Alto, CA, USA) for visual identification of transfected cells. The transfected cells were used 1–4 days after transfection, as sufficient protein was expressed for the electrophysiological measurements at this time.

Modelling

Due to the lack of a *K_v1.3* crystal structure, a homology model of the *K_v1.3* S4/S5/S6 domains was generated using the crystal structure of *K_v1.2* (PDB: 2A79) with 2.9 Å resolution as a template. All cysteine mutations were constructed by YASARA and the homology modelling was carried out by Dr Morteza Khabiri (Institute of Nanobiology and Structural Biology of GCRC Academy of Sciences of the Czech Republic). The three-dimensional (3D) model of MTSEA and verapamil was created by the Dundee Prodrug2 server (Schuettelkopf and van Aalten, 2004) on the basis of the chemical structure of these molecules. The final pdb files of these molecules were used for the docking process. These components were docked with the AutoDock 4.0 implementation (Krieger *et al.*, 2004) in YASARA (Krieger *et al.*, 2002). Initially, verapamil was positioned manually close to the equilibrated *K_v1.3* model struc-

ture based on the information from Rossokhin *et al.* (2011). Afterwards, MTSEA was docked into the channel model in the presence of verapamil. For visualization of the 3D structures of wt and mutant channels the Swiss PDB viewer and VMD 1.8.7 were used.

Materials

A stock solution of 1 M MTSEA reagent (Cat. No. A609100; Toronto Research Chemicals, Inc., North York, Canada) was prepared in distilled water and stored as aliquots at -20°C . They were diluted in the external bath solution to a final concentration of 1 mM directly before use. The phenylalkylamine verapamil (Sigma Aldrich Co, Munich, Germany) was dissolved in DMSO at a stock concentration of 100 mM and stored at $+4^{\circ}\text{C}$. It was diluted in the external bath solution to a final concentration of 100 μM directly before application. The bath solution could be completely exchanged by a manually, syringe-driven perfusion system allowing the complete exchange of the external bath solution within 10–20 s.

Results

In the current paper, three subsequent amino acids L418, T419 and I420 right after the residue V417 in the S6 segment were individually substituted by cysteines and the accessibility of these introduced cysteines was assessed by the externally applied MTSEA reagent. By using similar experimental procedures and voltage protocols as described for the *hK_v1.3_V417C* mutant channel (Schmid and Grissmer, 2011), the impact of MTSEA on these three *hK_v1.3* mutant channels (L418C, T419C and I420C) in the closed, open or inactivated states and in the presence of verapamil was monitored.

Effect of externally applied MTSEA on hK_v1.3 wt and hK_v1.3_L418C, hK_v1.3_T419C and hK_v1.3_I420C mutant channels in the closed and open states

In the present study, we confirmed the finding of Schmid and Grissmer (2011) that the *hK_v1.3* wt channel could not be

modified by externally applied MTSEA (Figure 1A). The currents through *hK_v1.3* wt and mutant channels (Figure 1) were recorded by depolarizing pulses from a holding potential of -120 to $+40$ mV for 200 ms, repeated every 30 s (for wt channels) or every 60 s (for mutant channels). As shown in Figure 1 (left column, trace a represents the current through the channels in a bath solution containing Na-Ringer), the current measured showed that *hK_v1.3* wt and mutant channels activated fast and reached a peak amplitude within ~ 18 ms with the peak current gradually decaying during the 200 ms voltage step (Table 1). Right after recording trace a, 1 mM MTSEA was added to the bath solution while the protocol was stopped and the membrane potential was held at -120 mV to make sure all channels were in the closed state. After 2 min, the step protocol was restarted again and 6–10 additional traces were recorded in the presence of MTSEA (only the first, second and last elicited currents are shown in Figure 1, left column).

Because MTSEA was added in the lag time between trace a and trace b, when channels were in the closed state, the first elicited current (trace b) after restarting the voltage steps should indicate the MTSEA effect on the closed state and the following traces (c and d) should demonstrate the effect of MTSEA on the open state of the channels. This specific pulsing procedure was developed (Schmid and Grissmer, 2011) and shown to eliminate problems associated with diffusion in the whole-cell mode as well as demonstrating that *hK_v1.3* wt channels cannot be modified in the closed state. For better visualization, we plotted the peak amplitudes of the elicited currents in Figure 1 (left column) against the recording time (Figure 1, right column). Figure 1 clearly shows that MTSEA had no effect on the closed state of *hK_v1.3* wt and mutant channels as traces a and b had similar peak current amplitudes. Comparing the peak currents in the presence of MTSEA (traces c and d) through wt channels (Figure 1A) with those through mutant channels (Figure 1B–D), it is obvious that wt channels were less modified by MTSEA. The results shown in Figure 1A confirm those reported by Schmid and Grissmer (2011). In contrast to wt channels, the current through mutant channels (Figure 1B–D, traces c and d) was reduced to zero during 4 min, indicating the modification of these mutant channels

Table 1

Intrinsic properties of the *hK_v1.3* wt and L418C, T419C and I420C mutant channels

		Wt- <i>hK_v1.3</i>	L418C	T419C	I420C
Activation	$V(a)_{1/2}$ (mV)	-40 ± 6.5	-35 ± 8.5	-38 ± 7.5	-37.6 ± 6.5
	k (mV)	8.2 ± 2.5	9.9 ± 1.9	8.6 ± 3	7.6 ± 2
Deactivation time constant (τ_d) at -60 mV (ms)		99 ± 11	81 ± 14	107 ± 14	88 ± 16
Inactivation time constant (τ_i) (ms)		294 ± 54	272 ± 35	344 ± 42	1018 ± 92
Recovery from inactivation (τ_{rec}) (s)		13 ± 1.5	25 ± 4	24 ± 3	22 ± 3
Verapamil K_D (μM)		8*	3.5	7.5	35
Time constant τ (s) of peak current loss in the presence of MTSEA		None	103 ± 14	83 ± 16	87 ± 16

All values are given as mean \pm SD; number of independent experiments is at least three. *Verapamil K_D value of wild type is from Rauer and Grissmer (1996).

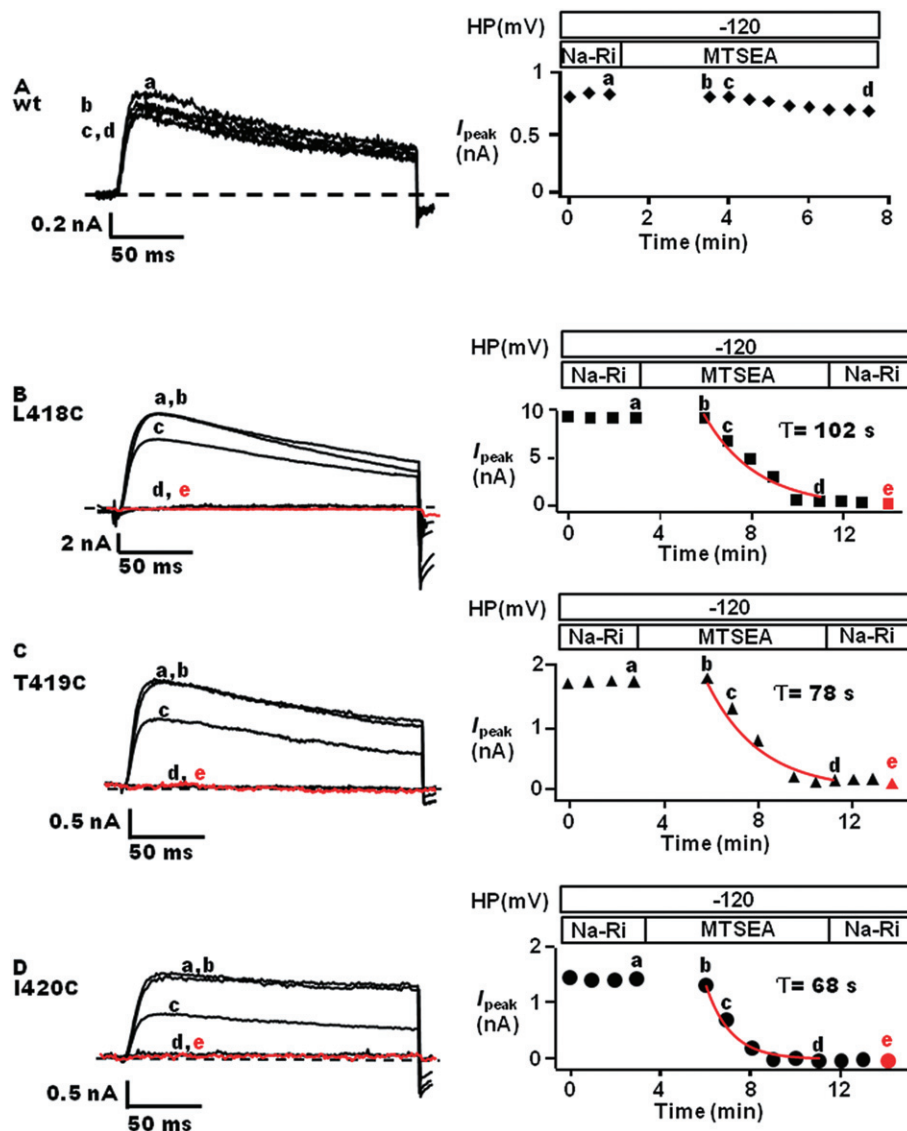


Figure 1

Effect of externally applied 1 mM MTSEA on current through (A) *hK_v1.3* wt channels, (B) *hK_v1.3_L418C*, (C) *hK_v1.3_T419C* and (D) *hK_v1.3_I420C* mutant channels in the closed and open states. The experiments were independently repeated five times ($n = 5$). (A–D, left) Representative whole-cell currents through the channels were elicited by 200 ms voltage pulses from -120 to $+40$ mV every 30 s (wt) or every 60 s (mutant channels). The currents were recorded before (trace a) and after adding 1 mM MTSEA (traces b–d) to the bath solution. Between traces a and b, the current recording was stopped and the membrane potential was held for 2 min at -120 mV. (A–D, right) The peak current amplitudes of the elicited currents from the experiment on the left were plotted against the recording time. The letters above the data points refer to the current traces shown on the left. The red lines are fits of exponential functions to the data points yielding time constants of peak current loss in the presence of MTSEA of 102 s (L418C), 78 s (T419C) and 68 s (I420C). HP, holding potential.

by MTSEA. To quantify this modification, we fitted exponential functions to the time course of the peak current reduction (Figure 1B–D, right column, red lines) and obtained time constants for this peak current loss of 102 s for the L418C mutant channels, 78 s for the T419C mutant channels and 68 s for the I420C mutant channels. In similar experiments, we obtained peak current loss time constants of 103 ± 14 s, 83 ± 16 s and 87 ± 16 s respectively (see also Table 1). To show the irreversible effect of MTSEA on these mutant channels, we washed out the MTSEA with Na-Ri directly after recording trace d. The washout did not result in any recovery

of current (Figure 1B–D, red traces e) and was similar to the reported current modification in the *hK_v1.3_V417C* mutant channel (Schmid and Grissmer, 2011).

*Modification of the inactivated state of *hK_v1.3_L418C*, *hK_v1.3_T419C* and *hK_v1.3_I420C* mutant channels by externally applied MTSEA*

Data presented in a previous study (Schmid and Grissmer, 2011) determined the ability of MTSEA to modify the

hKv1.3_V417C mutant channels in the inactivated state. We used the identical experimental and voltage step protocol conducted by Schmid and Grissmer (2011) to test whether the *hKv1.3_L418C*, *hKv1.3_T419C* and *hKv1.3_I420C* mutant channels could be also modified in the inactivated state. To determine that effect, MTSEA was added only when the mutant channels were in the inactivated state. To exclude artefacts, currents through the mutant channels were recorded first in the absence of MTSEA and then, using the same protocol in the same cell, in the presence of MTSEA. Therefore, the currents were recorded by 200 ms voltage pulses from -120 to $+40$ mV every 60 s (Figure 2A,C,E, black traces). Then the channels were inactivated by holding the membrane potential at -20 mV, for 1 min after stopping the pulse protocol. After 1 min at -20 mV, a 200 ms voltage step from this holding potential to $+40$ mV was recorded (Figure 2A,C,E, blue traces), this showed no current indicating that all mutant channels were in the inactivated state. Afterwards, the cells were washed twice with Na-Ri solution for 2 min while the membrane potential was kept at -20 mV. After the second wash, the membrane potential was switched from -20 to -120 mV and was maintained at -120 mV for 1 min in order for the channels to recover from the inactivated state. Afterwards, a 200 ms voltage step from this holding potential of -120 to $+40$ mV was elicited (Figure 2A,C,E, red traces), indicating a peak current almost identical to the trace recorded before the first wash (Figure 2A,C,E, black traces). These results suggest that holding the membrane potential for 1 min at -120 mV would be sufficient for these mutant channels to recover from the inactivation stimulated by the change of the holding potential to -20 mV. In the next step, cells were exposed to MTSEA using an identical protocol and holding potential adjustments. In place of washing-in Na-Ri, after the voltage pulse from -20 to $+40$ mV, 1 mM MTSEA was washed into the bath solution and maintained there for 2 min while the membrane potential was held at -20 mV. Then the MTSEA was washed out by Na-Ri. The currents elicited through all three mutant channels before the washing procedure (Figure 2B,D,F, black traces) were similar to the corresponding traces in the control test (Figure 2A,C,E, black traces). In addition, the currents recorded with the voltage pulses from -20 to $+40$ mV (Figure 2B,D,F, blue traces) were identical to the corresponding traces in the control experiments (Figure 2A,C,E, blue traces), indicating that most of the mutant channels were in the inactivated state. Comparing the current traces recorded through *hKv1.3_L418C* and *hKv1.3_T419C* mutant channels after treatment by MTSEA (Figure 2B,D, red traces) with the traces before (Figure 2A,C, black traces) showed that after treatment with MTSEA these mutant channels had almost fully recovered from inactivation (Figure 2B,D, left column, red traces) as these current traces were similar. Because the MTSEA modification is covalent and irreversible, the cysteine residues introduced into the *hKv1.3_L418C* and *hKv1.3_T419C* mutant channels were not modified by MTSEA in the inactivated state. These results in combination with data from Figure 1B,C allowed us to deduce that the closed and the inactivated states of the *hKv1.3_L418C* and *hKv1.3_T419C* mutant channels could not be modified by MTSEA and that the observed irreversible current reduction

in Figure 1B,C was due to the effect of MTSEA on the open state of these mutant channels. In contrast, the *hKv1.3_I420C* mutant channels in the inactivated state were irreversibly modified by MTSEA (Figure 2F, red trace), similar to the *hKv1.3_V417C* mutant channels reported by Schmid and Grissmer (2011).

*MTSEA modification of *hKv1.3_L418C*, *hKv1.3_T419C* and *hKv1.3_I420C* mutant channels in the presence of verapamil*

Schmid and Grissmer (2011) reported that verapamil could prevent the modification of *hKv1.3_V417C* mutant channels by MTSEA, indicating that verapamil binding to position A413 (Dreker and Grissmer, 2005) could partially cover position 417, thereby preventing MTSEA from reaching the cysteine residue at position 417. We were also interested in whether the MTSEA modification of *hKv1.3_L418C*, *hKv1.3_T419C* and *hKv1.3_I420C* mutant channels can be prevented by verapamil. For this purpose, we used the protocol described by Schmid and Grissmer (2011) to record the current through these three mutant channels. After recording a control current through the mutant channels (Figure 3, black traces), 100 μ M verapamil was added to the bath solution and the effects of verapamil on the mutant channels were characterized (for solution changes, see top of Figure 3, right column). For all three mutant channels, 100 μ M verapamil reduced the current as expected (Jacobs and DeCoursey, 1990; DeCoursey, 1995; Rauer and Grissmer, 1996). In the next step, a Na-Ri solution containing 100 μ M verapamil and 1 mM MTSEA was washed in as bath solution (Figure 3, left column, orange traces); this resulted in a further reduction of the current. Finally, first MTSEA and then verapamil were washed out by Na-Ri. Figure 3B,C (blue traces) showed that the currents through the *hKv1.3_T419C* and *hKv1.3_I420C* mutant channels recovered after the washout by Na-Ri, indicating that MTSEA could not modify those channels in the presence of verapamil. These results indicate that, similar to the *hKv1.3_V417C* mutant channel (Schmid and Grissmer, 2011), verapamil also prevented the MTSEA modification of the *hKv1.3_T419C* and *hKv1.3_I420C* mutant channels. Although we have no explanation as to why the recovery of current in the T419C mutant channels was less than in the I420C mutant channels, it is obvious that even the partial recovery indicates that verapamil prevented some modification.

In contrast, in the *hKv1.3_L418C* mutant channels, the current did not recover after removal of MTSEA and verapamil (Figure 3A, blue trace). This result suggests that the current through the *hKv1.3_L418C* mutant channels was irreversibly reduced by MTSEA even in the presence of verapamil. Therefore, verapamil could not prevent MTSEA from reaching the cysteine residue at position 418, and could not prevent the modification of *hKv1.3_L418C* mutant channels by MTSEA.

The data obtained from the present study and those reported by Schmid and Grissmer (2011) are summarized in Table 2, which shows the effect of MTSEA on four different mutant channels in different channel states and in the presence of verapamil.

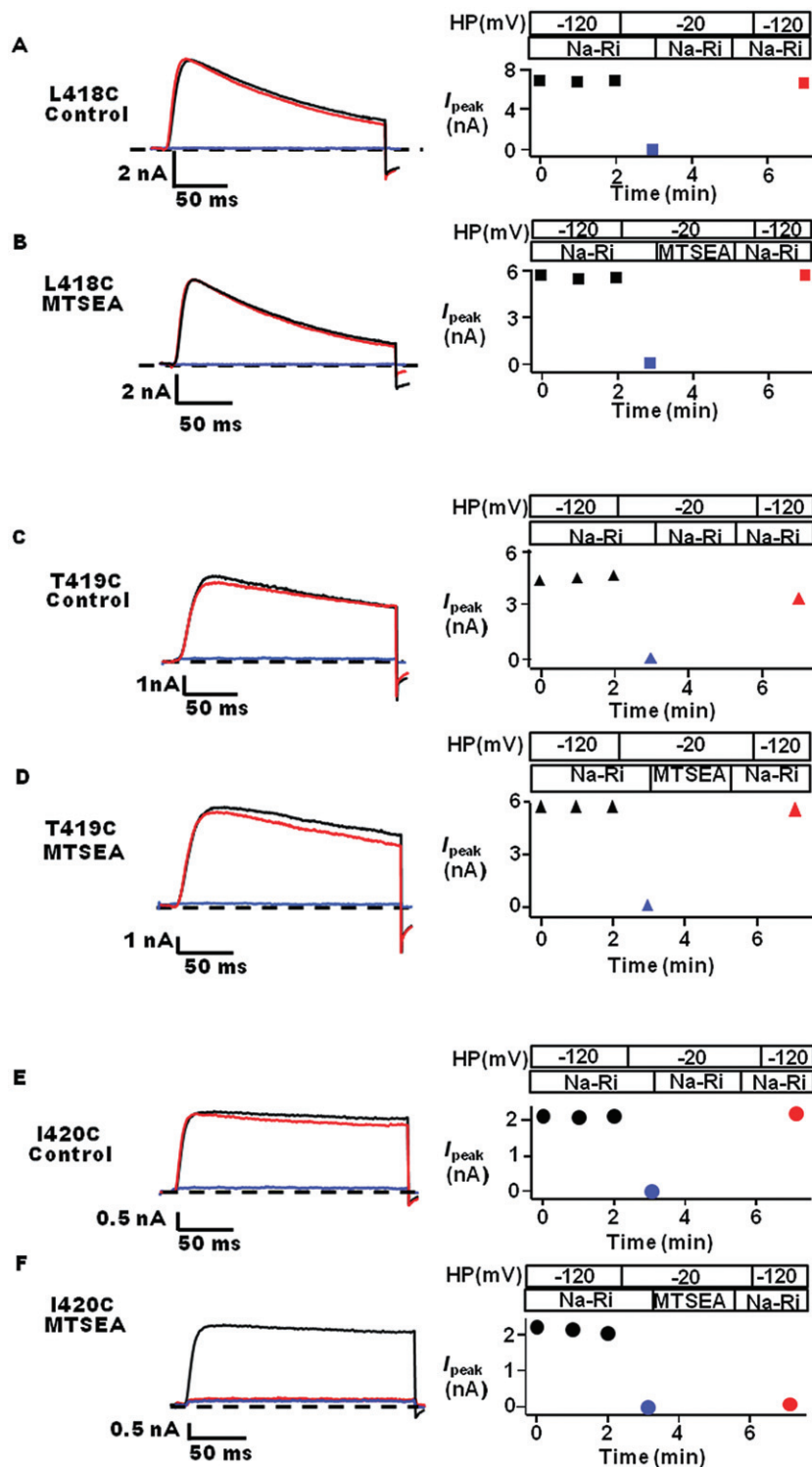


Figure 2

Effect of externally applied 1 mM MTSEA on the inactivated state of $hK_v1.3$ _L418C, $hK_v1.3$ _T419C and $hK_v1.3$ _I420C mutant channels. The experiments were independently repeated five times ($n = 5$). (A–F, left) Representative whole-cell currents were elicited by 200 ms voltage pulses from -120 to $+40$ mV every 60 s. After the black trace, the membrane potential was adjusted to -20 mV to ensure that all the mutant channels were in the inactivated state and a depolarizing step from this holding potential (HP) to $+40$ mV was applied (blue trace). After recording this trace, the solution was changed to Na-Ri (A,C,E) or MTSEA (B,D,F). After 2 min, the bath solution was replaced by Na-Ri and the membrane potential was adjusted to -120 mV again from which the next depolarizing voltage step to $+40$ mV was elicited (red trace). (A–F, right) Peak currents of the recorded traces shown on the left plotted against the recording time. Corresponding changes in the HP and solution changes are given in the boxes on top.

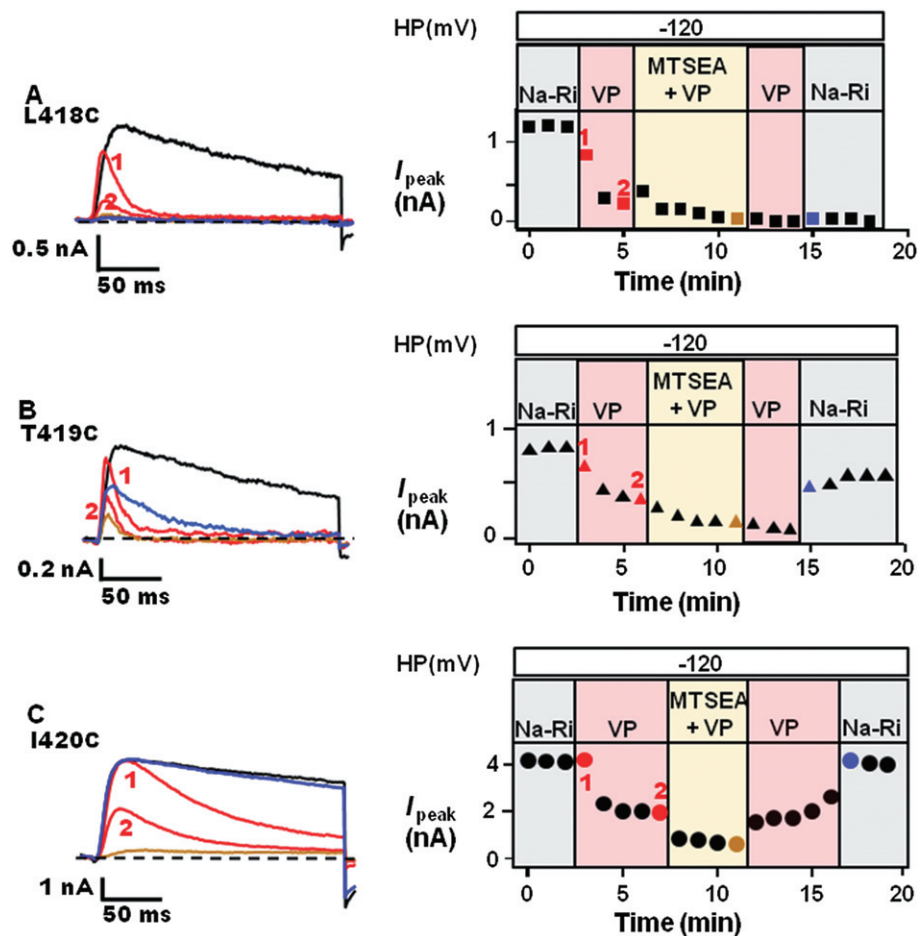


Figure 3

Possible protection against the effect of 1 mM MTSEA by the application of 100 μ M verapamil (VP) to the bath solution in $hK_v1.3_{L418C}$, $hK_v1.3_{T419C}$ and $hK_v1.3_{I420C}$ mutant channels. The experiments were independently repeated five times ($n = 5$). (A–C, left) Representative whole-cell currents were elicited by 200 ms depolarizing voltage steps from a holding potential (HP) of -120 to $+40$ mV every 60 s in different solutions as can be seen on the right side of the graph. (A–C, right) Peak current amplitudes of the currents elicited in the experiment on the left were plotted against the recording time. After having recorded three control traces in a bath solution containing Na-Ri, the bath solution was replaced several times: firstly, by a Na-Ri solution containing 100 μ M VP; secondly, by a Na-Ri solution containing 100 μ M VP + 1 mM MTSEA (MTSEA + VP); thirdly, by a Na-Ri solution containing 100 μ M VP; and finally, by a Na-Ri solution as in the beginning (Na-Ri) of the experiment. The letters above the points refer to the current traces shown on the left.

Table 2

Summary of the effect of MTSEA on four different mutant channels in different channel states and in the presence of verapamil (with VP)

Mutant channel	Channel state			
	Open	Inactivated	Closed	With VP
$hK_v1.3_{V417C}$ *	+	+	–	–
$hK_v1.3_{L418C}$	+	–	–	+
$hK_v1.3_{T419C}$	+	–	–	–
$hK_v1.3_{I420C}$	+	+	–	–

*Data reported by Schmid and Grissmer (2011).

+ Channel modified by MTSEA, – channel not modified by MTSEA.

Discussion

The present paper confirms and extends the effects of MTSEA on the *hK_v1.3_V417C* mutant channels in different states and in the presence of verapamil determined previously (Schmid and Grissmer, 2011). In the present study, we tested the amino acid residues from L418 to I420, right after the V417 residue, and confirmed that MTSEA hardly reduces the current through wt *hK_v1.3* channels.

MTSEA could not modify the hK_v1.3_L418C, hK_v1.3_T419C and hK_v1.3_I420C mutant channels in the closed state

Our observations (shown in Figure 1B–D) suggest that the *hK_v1.3_L418C*, *hK_v1.3_T419C* and *hK_v1.3_I420C* mutant channels are not modified by MTSEA in the closed state. This result is in agreement with the effect of MTSEA on *hK_v1.3_V417C* mutant channels (Schmid and Grissmer, 2011) and *Shaker* channels with cysteines introduced at positions 470, equivalent to I420 in the *hK_v1.3* channel (Liu *et al.*, 1997). Based on the location of the activation gate in *Shaker* channels from previous studies (Liu *et al.*, 1997; del Camino and Yellen, 2001), we conclude that the residues L418–I420 (468–470 in *Shaker*) are located behind the activation gate and this might explain why the cysteines in positions V417–I420 in the *hK_v1.3* mutant channels could not be modified by MTSEA in the closed state.

MTSEA modification of hK_v1.3_L418C, hK_v1.3_T419C and hK_v1.3_I420C mutant channels in the open and inactivated states

In this study, we demonstrated that, similar to *hK_v1.3_V417C* mutant channels (Schmid and Grissmer, 2011), the cysteine at position 420 of *hK_v1.3_I420C* mutant channels could be modified by MTSEA in the inactivated state (Figure 2E,F). The two cysteines at positions 418 and 419, located between V417 and I420, were not accessible to MTSEA in the inactivated state (Figure 2A–D), but all four cysteines (417–420) could be modified in the open state. These results indicate that the opening of the activation gate is necessary for MTSEA to access the cysteines at positions 417–420. The results also imply that in the inactivated state the activation gate was open. These findings are consistent with the recent model of the *KcsA* channel, which demonstrates the open bundle crossing (activation gate) in the inactivated channel (Cuello *et al.*, 2010a,b). A comparison of the accessibility of residues 417–420 in the open and inactivated states (Table 1) revealed that residues 417 and 420 were available in the open and inactivated states but residues 418 and 419 were only accessible in the open state. The simplest explanation for this different accessibility of residues 417–420 in the open and inactivated states is a structural rearrangement of the S6 segment or other parts of the channel during inactivation causing residues 418 and 419 to be covered. These findings confirm the results observed with *Shaker* channels by Panyi and Deutsch (2007). Although we cannot distinguish whether the S6 segment or other parts of the channel moves during inactivation, a relative movement in the vicinity of residues 418 and 419 during inactivation is inevitable, as has

been suggested by Cuello *et al.* (2010a,b) for C-type inactivation in *KcsA* channels. Their model suggests that structural rearrangements, such as hinge bending and rotation of the TM₂ helix (equivalent to the S6 helix in the *K_v1.3* channel), lead to C-type inactivation.

Verapamil protects the hK_v1.3_T419C and hK_v1.3_I420C mutant channels from MTSEA modification but not the hK_v1.3_L418C

As previously demonstrated, verapamil prevented the MTSEA-induced modification of *hK_v1.3_V417C* mutant channels (Schmid and Grissmer, 2011). To follow up these results, we performed similar blocker protection experiments to determine the accessibility of the cysteines at positions 418–420 to MTSEA in the presence of verapamil. It was expected that, similar to the *hK_v1.3_V417C* mutant channels, verapamil would also prevent the modification of the *hK_v1.3_L418C*, *hK_v1.3_T419C* and *hK_v1.3_I420C* mutant channels by MTSEA, as the L418, T419 and I420 amino acids are just next to the V417 in the S6 helix. Surprisingly, the cysteine at position 418 was modified by MTSEA even in the presence of verapamil, even though verapamil protect the amino acids located above (417C) and below (419C, 420C) residue 418 (Figure 3, Table 1).

Why did verapamil fail to protect the cysteine at position 418 from MTSEA modification? To address this question, we used a 3D model of the tetrameric *K_v1.3* channel to show the spatial arrangement of these residues. Because the *hK_v1.3* has not been crystallized yet, the crystal structure of *K_v1.2* with a sequence identity over 90% to *K_v1.3* was used to prepare a reasonable structural model. Therefore, a homology model of the *K_v1.3* S4/S5/S6 domains was generated using the crystal structure of *K_v1.2* (PDB: 2A79) as a template. The positions of amino acids (V417–I420) are shown in Figure 4; this demonstrates that residues V417–I420 construct one helical turn of the S6 α -helix. Two residues V417 and I420 are located on the helical turn towards the centre of the inner pore, the other residues L418 and T419 are located on the other side of the helical turn. Although L418 and T419 are located on the outside of the helical turn, both of these residues can sense the environment of the inner pore in the open state.

Verapamil was docked into the channel (Figure 5) according to Rossokhin *et al.* (2011). The ammonium group of verapamil was manually placed near the backbone carbonyl of T391 at the P-turn. The residues M390 and A413 provide a hydrophobic place in close contact with the phenylethylamine meta- and para-methoxy groups of verapamil whereby the other moiety of the verapamil molecule (pentanenitriphenyl) might physically block the pore. The inset highlights the close-up view of verapamil and residues 417–420 in S6 of one monomer. This view shows that verapamil is located in the upper part of the cavity and that residues at position 417 and 420 can be shielded by verapamil, whereas the residues at positions 418 and 419 are facing away from verapamil (Figure 5). The blocker protection assay showed that the cysteines at positions 417, 419 and 420 could not be modified by MTSEA in the presence of verapamil. It seems that verapamil, after binding to the presumed position A413 (Dreker and Grissmer, 2005), could partially cover the cysteines at positions 417 (Schmid and Grissmer, 2011) and 420, thereby preventing its modification by MTSEA, because

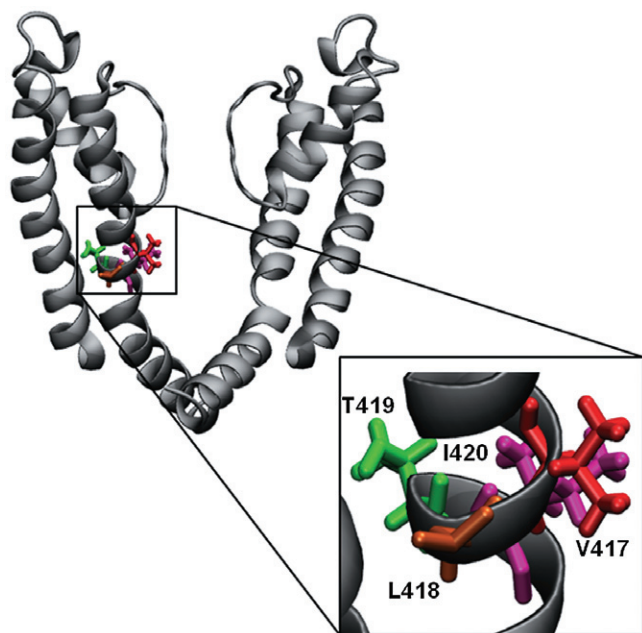


Figure 4

Side view of two monomers of the $K_v1.3$ channel highlighting the amino acid residues in the α -helix of a single S6 segment that were mutated to cysteines. For reasons of clarity, just S5–S6 of each monomer is shown in this picture. The inset highlights the close-up view of residues in S6 that were substituted to cysteines in our experiments. Molecular graphic images were produced by using VMD1.8.7 software.

both residues are facing towards verapamil (Figure 5). Although residue 419 was not covered by verapamil (Figure 5), it was protected from modification by MTSEA, suggesting that verapamil physically blocks the inner pore thereby blocking the pathway for MTSEA to reach position 419.

In contrast to residue 419, residue 418 could not be protected by verapamil from MTSEA modification. We were interested in elucidating how MTSEA reaches the cysteine at position 418 even in the presence of verapamil. For this purpose, MTSEA was docked into the $hK_v1.3_{L418C}$ mutant channel in the presence of verapamil (Figure 6). This figure clearly shows that in the presence of verapamil there is enough space for MTSEA to be close to the residue at position 418. Therefore, there seems to be no interference between the location of verapamil and the interaction of MTSEA with position 418. This means that the simultaneous presence of verapamil and MTSEA is possible, and therefore MTSEA can reach and bind to the residue at position 418 even in the presence of verapamil. Thus, the model presented in Figure 6 could explain the results obtained in our experiments regarding position 418. Although there also seems to be enough space for the interaction of MTSEA with position 419 in the presence of verapamil, the experimental data argue against such a possibility.

Conclusion

In conclusion, the cysteine at position 420 was modified by MTSEA in the open and the inactivated states, while the residues at positions 418 and 419 were modified only in the open state. Verapamil could not prevent MTSEA reaching residue 418 but protected the residues 419 and 420 from

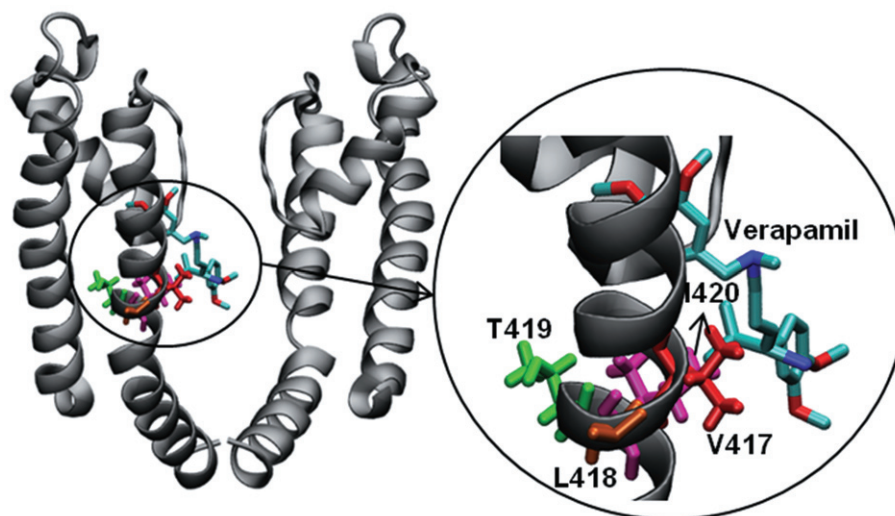


Figure 5

Docking of verapamil into a homology model of the $hK_v1.3$ channel. The representative $hK_v1.3$ channel structure is composed of two monomers and each monomer includes S5, S6; and the P-turn is shown in grey. The inset highlights the close-up of the positions of verapamil and residues in S6, which were substituted in our experiment. The residues in one monomer have been shown in different colours (V417: red, L418: orange, T419: green, I420: magenta).

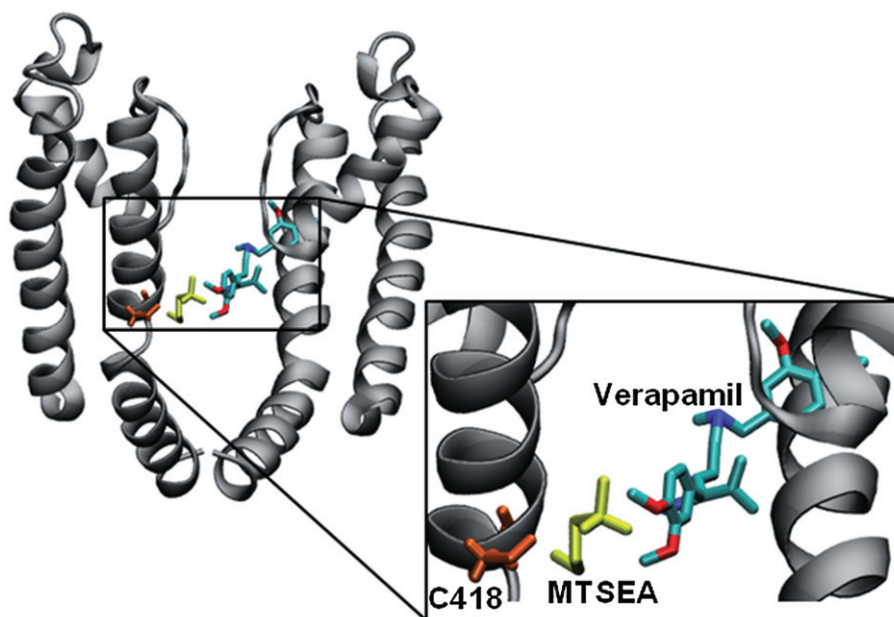


Figure 6

Docking of MTSEA into the $hK_v1.3$ _L418C mutant channel in the presence of verapamil. Two monomers of the channel are shown in grey, position 418 is shown in orange. The inset highlights the close-up view of the positions of verapamil, MTSEA (yellow) and residue C418 (orange) in S6.

MTSEA modification. It seems that the movement of the S6 segment during inactivation did not cause a movement of the side chain of residues 417 (Schmid and Grissmer, 2011) and 420 in a way that they are not lining the pore any more, but it led to the inaccessibility of the residues at positions 418 and 419. The difference in the modification of these cysteine residues demonstrated the changes in accessibility of these residues during different conformations of the $hK_v1.3$ channel. This has implications for the 3D structure of the channel in different states especially in the C-type inactivated state, a state specific for $hK_v1.3$ channels (Hanner *et al.*, 1999), thereby facilitating the rational design of drugs useful for the treatment of autoimmune diseases.

Acknowledgements

The authors would like to thank Ms Katharina Ruff for her excellent technical assistance. We thank Prof Dr O. Pongs who generously gave us the plasmid for the wild-type $hK_v1.3$ channel; and Dr Tobias Dreker who introduced the L418C, T419C and I420C point mutations in the $hK_v1.3$ channel. We also thank Dr Morteza Khabiri for his help to make the homology model. This work was supported by grants from the Deutsche Forschungsgemeinschaft (Gr 848/14-1 and 16-1) to S. G.

Conflict of interest

None.

References

- Choi KL, Aldrich RW, Yellen G (1991). Tetraethylammonium blockade distinguishes two inactivation mechanisms in voltage-activated K^+ channels. *Proc Natl Acad Sci USA* 88: 5092–5095.
- Cordero-Morales JF, Cuello LG, Zhao Y, Jogini V, Cortes DM, Roux B *et al.* (2006). Molecular determinants of gating at the potassium-channel selectivity filter. *Nat Struct Mol Biol* 13: 311–318.
- Cuello LG, Jogini V, Cortes DM, Perozo E (2010a). Structural mechanism of C-type inactivation in K^+ channels. *Nature* 446: 203–209.
- Cuello LG, Jogini V, Cortes DM, Pan AC, Gagnon DG, Dalmas O *et al.* (2010b). Structural basis for the coupling between activation and inactivation gates in K^+ channels. *Nature* 466: 272–275.
- DeCoursey TE (1995). Mechanism of K^+ channel block by verapamil and related compounds in rat alveolar epithelial cells. *J Gen Physiol* 106: 745–779.
- DeCoursey TE, Chandy KG, Gupta S, Cahalan MD (1984). Voltage-gated K^+ channels in human T lymphocytes: a role in mitogenesis? *Nature* 307: 465–468.
- Del Camino D, Yellen G (2001). Tight steric closure at the intracellular activation gate of a voltage-gated K^+ channel. *Neuron* 32: 649–656.
- Dreker T, Grissmer S (2005). Investigation of the phenylalkylamine binding site in $hK_v1.3$ (H399T), a mutant with a reduced C-type inactivated state. *Mol Pharmacol* 68: 966–973.
- Grissmer S, Cahalan M (1989). TEA prevents inactivation while blocking open K^+ channels in human T lymphocytes. *Biophys J* 55: 203–206.

- Grissmer S, Dethlefs B, Wasmuth JJ, Goldin AL, Gutman GA, Cahalan MD *et al.* (1990). Expression and chromosomal localization of a lymphocyte K⁺ channel gene. *Proc Natl Acad Sci USA* 87: 9411–9415.
- Hamill OP, Marty A, Neher E, Sakmann B, Sigworth FJ (1981). Improved patch-clamp techniques for high-resolution current recording from cells and cell-free membrane patches. *Pflügers Arch* 391: 85–100.
- Hanner M, Schmalhofer WA, Green B, Bordallo C, Liu J, Slaughter RS *et al.* (1999). Binding of correolide to K(v)1 family potassium channels. Mapping the domains of high affinity interaction. *J Biol Chem* 274: 25237–25244.
- Hanner M, Green B, Gao YD, Schmalhofer WA, Matyskiela M, Durand DJ *et al.* (2001). Binding of correolide to the K(v)1.3 potassium channel: characterization of the binding domain by site-directed mutagenesis. *Biochemistry* 40: 11687–11697.
- Jacobs ER, DeCoursey TE (1990). Mechanisms of potassium channel block in rat alveolar epithelial cells. *J Pharmacol Exp Ther* 255: 459–472.
- Kiss L, Korn SJ (1998). Modulation of C-type inactivation by K⁺ at the potassium channel selectivity filter. *Biophys J* 74: 1840–1849.
- Krieger E, Koraimann G, Vriend G (2002). Increasing the precision of comparative models with YASARA NOVA – a self-parameterizing force field. *Proteins* 47: 393–402.
- Krieger E, Darden T, Nabuurs SB, Finkelstein A, Vriend G (2004). Making optimal use of empirical energy functions: force field parameterization in crystal space. *Proteins* 57: 678–683.
- Lenaeus MJ, Vamvouka M, Focia PJ, Gross A (2005). Structural basis of TEA blockade in a model potassium channel. *Nat Struct Mol Biol* 12: 454–459.
- Liu Y, Holmgren M, Jurman ME, Yellen G (1997). Gated access to the pore of a voltage-dependent K⁺ channel. *Neuron* 19: 175–184.
- Long SB, Campbell EB, MacKinnon R (2005a). Crystal structure of a mammalian voltage-dependent *Shaker* family K⁺ channel. *Science* 309: 897–903.
- Long SB, Campbell EB, MacKinnon R (2005b). Voltage sensor of K_v1.2: structural basis of electromechanical coupling. *Science* 309: 903–908.
- Panyi G, Deutsch C (2007). Probing the cavity of the slow inactivated conformation of *Shaker* potassium channels. *J Gen Physiol* 129: 403–418.
- Rauer H, Grissmer S (1996). Evidence for an internal phenylalkylamine action on the voltage-gated potassium channel K_v1.3. *Mol Pharmacol* 50: 1625–1634.
- Rauer H, Grissmer S (1999). The effect of deep pore mutations on the action of phenylalkylamines on the K_v1.3 potassium channel. *Br J Pharmacol* 127: 1065–1074.
- Rossokhin A, Dreker T, Grissmer S, Zhorov B (2011). Why does the inner-helix mutation A413C double the stoichiometry of K_v1.3 channel block by emopamil but not by verapamil? *Mol Pharmacol* 79: 681–691.
- Schmid SI, Grissmer S (2011). Effect of verapamil on the action of methanethiosulfonate reagents on human voltage-gated K_v1.3 channels: implications for the C-type inactivated state. *Br J Pharmacol* 163: 662–674.
- Schuettelkopf AW, van Aalten DMF (2004). PRODRG – a tool for high-throughput crystallography of protein-ligand complexes. *Acta Crystallogr D Biol Crystallogr* 60: 1355–1363.
- Yellen G, Sodickson D, Chen T, Jurman ME (1994). An engineered cysteine in the external mouth of a K⁺ channel allows inactivation to be modulated by metal binding. *Biophys J* 66: 1068–1075.